Available online at www.sciencedirect.com

Journal of Catalysis 238 (2006) 46–57

JOURNAL OF CATALYSIS

www.elsevier.com/locate/jcat

Highly efficient catalytic conversion of chloromethane to light olefins over HSAPO-34 as studied by catalytic testing and in situ FTIR

Yingxu Wei [a,b], Dazhi Zhang [b], Zhongmin Liu [b,*], Bao-Lian Su [a,*]

[a] *Laboratoire de Chimie des Matériaux Inorganiques (CMI), ISIS, The University of Namur (FUNDP), 61 rue de Bruxelles, B-5000 Namur, Belgium*
[b] *Natural Gas Utilization and Applied Catalysis Laboratory, Dalian Institute of Chemical Physics, Chinese Academy of Sciences, P.O. Box 110, 116023 Dalian, PR China*

Received 2 June 2005; revised 11 November 2005; accepted 20 November 2005

Abstract

The catalytic conversion of chloromethane over HSAPO-34 was followed by in situ Fourier transform infrared (FTIR) spectroscopy and catalytic testing. Our detailed IR investigation allowed the identification of the active sites and the adsorbed species. HSAPO-34 has high activity and selectivity for the production of light olefins. The FTIR results demonstrated that the conversion starts at 350 °C with the formation of alkoxy groups as intermediate products. On adsorption and conversion of chloromethane, three distinct shifts of –OH bands associated with the Si(OH)Al acidic sites were observed, attributed to the interaction between Si(OH)Al with CH_3Cl, HCl and C=C groups. In the 350–500 °C temperature range, chloromethane is converted to ethylene, propylene, and butylenes with 70–80% selectivity. Increasing reaction temperature increases conversion and enhances the yield of lighter olefins. The detailed FTIR study of chloromethane conversion at 450 °C at different system chloromethane loadings reveals that increasing system CH_3Cl loading increased the conversion rate. This is attributed to the participation of gas-phase chloromethane molecules with adsorbed species enhancing the reaction rate, while at lower chloromethane loadings, the reactions may just occur between the adsorbed species. The IR studies also reveal the reversible breaking of Al–O–P bonds on adsorption of HCl, a main product of the reaction, to generate large amounts of P–OH groups. The Al–O–P bonding was restored after removal of HCl by evacuation at 150 °C. These IR observations combined with the catalytic test results allow us to propose a realistic reaction mechanism.

Keywords: SAPO-34; Chloromethane conversion; FTIR; Catalytic testing; Light alkenes; HCl; Reaction mechanism

1. Introduction

Rational and efficient conversion of methane to more useful higher hydrocarbons is one of the most important topics in natural gas utilization. Although methane activation and its direct conversion to valuable compounds are attracting increasing attention, methane conversion is often made in indirect way, such as through transformation of methane to syngas (a mixture of CO, CO_2, and hydrogen) by steam-reforming over nickel-supported catalyst, after which the syngas can be converted to hydrocarbons (gasoline or olefins) using Fischer–Tropsch catalysis. Another process concerns the conversion of syngas first to methanol using $Cu/ZnO/Al_2O_3$ catalyst and then to hydrocarbons using MTO or MTG catalyst [1–4].

It is well known that although the Fischer–Tropsch process can effectively produce high hydrocarbons from syngas, a wide range of hydrocarbons is obtained. Producing a single organic compound with high selectivity is difficult, maybe even impossible, at least at the moment. The development of alternative routes for higher hydrocarbons production through methane transformation is a topic of much interest for industry and academia. It remains a great challenge as we face the sharp and ceaseless increase in the price of crude oil, due to the growing need for a series of organic compounds as starting reagents for pharmaceutical, plastic and fine chemical industries.

Some promising results have appeared to be of great importance in the catalytic conversion of chloromethane to higher hydrocarbons. In 1985, Olah and coworkers described a very

---

[*] Corresponding authors. Fax numbers: +86 411 84691570, +32 81 725414.
E-mail addresses: zml@dicp.ac.cn (Z. Liu), bao-lian.su@fundp.ac.be (B.-L. Su).

0021-9517/$ – see front matter © 2005 Elsevier Inc. All rights reserved.
doi:10.1016/j.jcat.2005.11.021

interesting and attractive three-step catalysis process for the transformation of methane to higher hydrocarbons through halide methane: monohalogenation of methane by a very simple method to halide methane, hydrolysis of halide methane to methanol, and then the MTG reaction on HZSM-5 [5]. In 1988, Taylor et al. invented a cycle process on the basis of their research results for the production of gasoline from methane with chloromethane as the intermediate [6]. Compared with the work of Olah and coworkers, the transformation from methane to gasoline was reduced to two stages: oxyhydrochlorination (OHC) for the production of chloromethanes from methane and MTG for the direct transfer of methyl chloride to gasoline with a byproduct of HCl, which can be recycled for the first step. This is a quite innovative and realistic process that can be really applicable in industry. The corrosion problem of HCl production can be resolved. For chloromethane transformation, HZSM-5 appears to be the most promising zeolite catalyst [7,8]. Recent work [9,10] has shown that the large-pore zeolite catalysts in both cationic and protonic forms, such as X, Y, EMT, Beta, and MOR, despite their very interesting activity, led to the formation of large amounts of coke in chloromethane conversion due to the large cages or channels present in these zeolites. In contrast, medium-pore ZSM-5 zeolite catalysts in either cationic or protonic form demonstrated high activity and long life in the reaction and strongly reduced coke formation. Some modifications to zeolite catalysts further improved the activity and selectivity of the reaction. For example, Mg- or P-modified ZSM-5 catalysts showed high selectivity for the formation of light olefins [11]. All of these works indicated that, like the renowned MTO and MTG processes, chloromethane transformation to higher hydrocarbons potentially could be an efficient alternative route for methane utilization using a cycle process, as proposed by Taylor et al.

There are undoubtedly many parallels between the reactions of CH_3Cl and CH_3OH transformation to higher hydrocarbons [9,10,12–16]. The important distinction between chloromethane and methanol transformation is that the proposed intermediates derived from CH_3OH, such as CH_3OCH_3, are not accessible in CH_3Cl conversion. For chloromethane transformation, methoxy group is considered the intermediate [10,14,15]. Some mechanisms for the first C–C bond formation have been pointed out in the study of chloromethane transformation over cation-exchanged zeolite catalyst [10].

Compared with a large series of work carried out with classical cationic and protonic zeolites, the SAPO-type molecular sieve catalyst, with excellent performance in catalytic conversion of methanol to light olefins [17–19], has seemingly been neglected up to now in the research of chloromethane conversion. SAPO-34 has shown its superiority in the MTO process and could be a very promising catalyst for chloromethane conversion to other hydrocarbons, especially to light olefins, such as ethylene and propylene, due to its small channel size. In regard to the difference in chemical composition between classical zeolites and SAPO molecular sieves, the nature of the active sites and the activation and transformation of chloromethane on SAPO-34 should be quite different and merit a detailed investigation.

In this study, SAPO-34 was used as the catalyst for chloromethane conversion for the first time. This conversion was carried out in a fixed-bed reactor and followed by in situ Fourier transform infrared (FTIR) spectroscopy. The conversion at different temperatures and different loadings of chloromethane was studied. Our aim was not only to study the catalytic behavior of SAPO-34 to determine the effect of different reaction conditions on chloromethane conversion to this catalyst, but also to shed some light on the reaction mechanism.

2. Experimental

2.1. Synthesis of SAPO-34

SAPO-34 was synthesized by the hydrothermal method as described in the literature [20] from a gel composition of 3.0 R:1.0 P_2O_5:1.0 Al_2O_3:0.8 SiO_2:50 H_2O, where R is triethylamine as the template. Pseudoboehmite, orthophosphoric acid (85 wt%), and colloidal silica were used as the sources of aluminum, phosphorus, and silicon, respectively. To prepare the starting gel, the pseudoboehmite was mixed with orthophosphoric acid and distilled water while stirring at room temperature for 2 h. Triethylamine and colloidal silica were subsequently added to this gel, and then the mixture was stirred continuously for another 2 h. The gel was sealed in a stainless-steel, polytetrafluoroethylene (PTFE)-lined autoclave. After letting the gel age at room temperature for 12 h, the autoclave containing the gel was heated at 200 °C for 24 h under autogenic pressure. The products were filtered, washed, and dried at 110 °C for 3 h, then calcined in air at 550 °C for 6 h to completely remove the template.

The multi-technique characterization of SAPO-34 has been reported elsewhere [21]. The chemical composition of synthesized SAPO-34 after removal of organic template is $Al_{0.49}P_{0.41}Si_{0.10}O_2$.

2.2. In situ FTIR study

Self-supported SAPO-34 wafers ($17\ mg/cm^2$) were first calcined in a flow of dry oxygen at 450 °C for 10 h and then in vacuum for 4 h. After cooling to room temperature, the spectra of SAPO-34 phase and gas phase were recorded using a Fourier transform spectrometer as reference (Perkin–Elmer Spectrum 2000). The wafers were put in contact with known amount of CH_3Cl. The chloromethane was purchased from Aldrich Chemical Company (99.5%). As for the effect of temperature, the conversion of chloromethane was performed in situ at reaction temperatures ranging from 250 to 500 °C for 15 min with a system chloromethane loading of 45 molecules per unit cell (m/uc). For the effect of chloromethane loading, the conversion was carried out at 450 °C for 5, 15, 30 and 60 min with chloromethane loadings of 15, 30, 45, and 60 m/uc, respectively. After reaction, the samples were cooled in liquid nitrogen to stop the reaction, and the IR spectra of gas phase in the IR cell and adsorbed phase with the catalyst were recorded.

2.3. Catalytic testing

The catalytic tests were performed using a fixed-bed reactor system at atmospheric pressure. First, 0.62 g of catalyst was loaded into a quartz reactor with an inner diameter of 5 mm. The sample was pretreated in a flow of dry nitrogen at 500 °C for 1 h, after which the atmosphere was replaced by nitrogen and chloromethane (with a N_2/CH_3Cl molar ratio of 1), and the reactor temperature was adjusted as desired in the range of 350–500 °C. Fresh catalyst was used for each temperature measurement. The weight hourly space velocity was 3.17 h^{-1} for chloromethane. The product stream was kept at 180 °C and analyzed on-line using a Varian GC3800 gas chromatograph equipped with a flame ionization detector and a PONA capillary column.

3. Results and discussion

3.1. Catalytic testing

The effect of reaction temperature on chloromethane conversion and selectivity of the products was studied by catalytic testing; the results are given in Figs. 1–3. Fig. 1 shows the temperature dependence of the conversion. A conversion of 70% is reached at 500 °C. Fig. 2 gives the product distribution in carbon number. It is quite interesting to observe that C_2–C_4 hydrocarbons are the main products of this reaction. This is significantly different from the products obtained on a series of large-pore zeolite catalysts, such as X, Y, EMT, Beta and MOR [9,10,16] and should be attributed to the eight-ring pore structure of SAPO-34. The narrow pore opening favors the production of light hydrocarbons and prohibits the desorption of larger hydrocarbon molecules out of the window, such as aromatic and hydrocarbons higher than C_6. The higher temperature favors the generation of smaller products. In fact, at relatively low reaction temperature, the formation of C_3 products (propylene and propane) predominates. At 450 °C, the selectivity of C_2 and C_3 attain the same level, whereas at 500 °C, the C_2 products predominate. Methane production increases slightly with increasing reaction temperature, which may result from cracking of the hydrocarbon products.

The distribution of the products as a function of reaction temperature is detailed in Fig. 3. Light alkenes, such as ethylene, propylene and butenes, are the main products of the reaction in the temperature range studied. At any reaction temperature, almost 80% of the products are attributed to ethylene, propylene, and butenes, indicating that SAPO-34 is a very selective catalyst for the production of light alkenes. With increasing reaction temperature, the selectivity of ethylene increases and that of propylene and butenes decreases. The highest ethylene selectivity (40%) in the studied reaction temperature range can be obtained at 500 °C. Only a small amount of light alkanes can be observed at 350–450 °C. The products heavier than C_5 account for 15–20% of all products in this temperature range, which may result from the oligomerization of light alkenes or the alkylation of light alkanes with alkenes. At 500 °C, methane becomes more prominent than other light alkanes, possibly

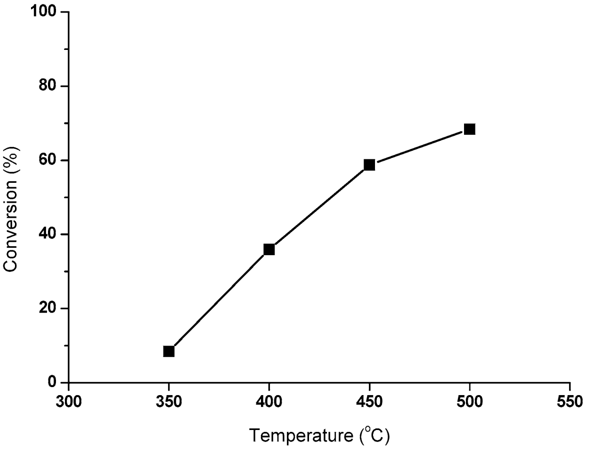

Fig. 1. Chloromethane conversion at different temperatures.

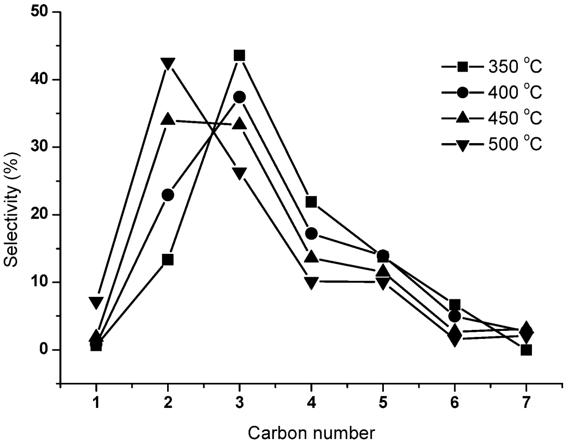

Fig. 2. Carbon number distribution of chloromethane conversion at different temperatures.

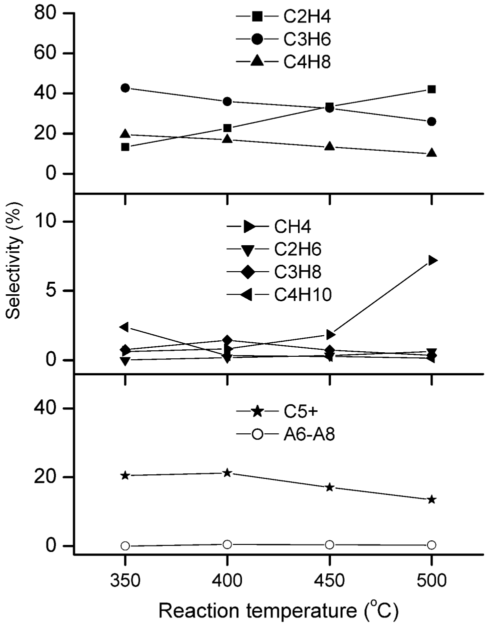

Fig. 3. Products distribution of chloromethane conversion over SAPO-34 at different temperatures.

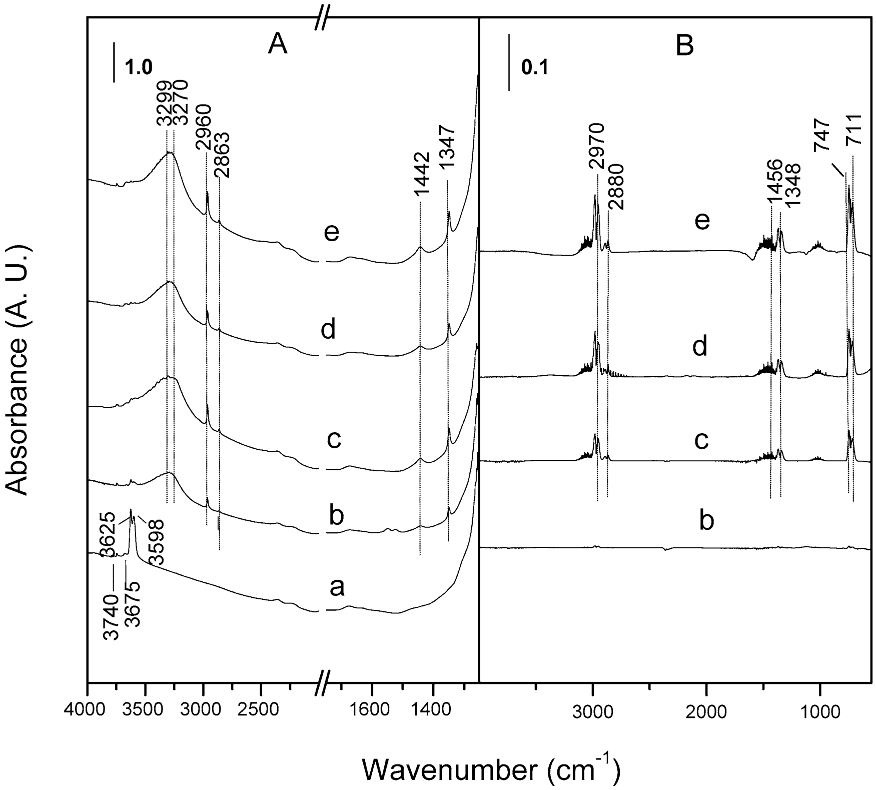

Fig. 4. FTIR spectra of adsorption of chloromethane on activated SAPO-34 (A) and the gas phase of the IR cell (B). (a) Activated SAPO-34 and system chloromethane loading (m/uc) of 15 (b), 30 (c), 45 (d) and 60 (e).

from cracking favored thermodynamically by the high temperature. This was previously observed with other zeolite catalysts [9,10,16]. Only trace amounts of aromatic products were observed over the temperature range studied. This is very different from chloromethane transformation over ZSM-5 catalyst, with alkane and aromatics as the main products. The cages of SAPO-34 does not prohibit the formation of aromatics, but the eight-ring pore opening prohibits the desorption of aromatics. During the reaction, HCl is also observed in the products (but is not listed in the product distribution).

3.2. *FTIR study*

3.2.1. *Surface hydroxyls of SAPO-34 and adsorption of chloromethane*

Fig. 4 gives the spectra of activated SAPO-34 and adsorption of chloromethane with different system loadings. The spectra in Fig. 4A represent only the species adsorbed on the SAPO-34 phase with the gas phase subtracted, whereas the spectra in Fig. 4B describe the gas phase present in the IR cell. After activation, SAPO-34 gives four peaks in the range of 3000–4000 cm^{-1} representing four types of hydroxyl groups (Fig. 4Aa). Two peaks at 3625 and 3598 cm^{-1} can be attributed to two types of Si(OH)Al groups differed in their localization. The bridged group with $\upsilon = 3598$ cm^{-1} is assumed to be localized in the hexagonal prism, forming an H-bond with adjacent oxygen atoms of the framework whereas the isolated bridged OH groups pointing toward the center of the elliptical cages give a vibration frequency at 3625 cm^{-1} [22–25]. These two types of OH groups are considered to have similar acidic properties and to be the active sites for acid-catalyzing reaction [26,27]. The other two peaks at 3675 and 3743 cm^{-1}, with very low intensity, are assigned to P–OH and Si–OH, respectively, which are generated by the defect sites of SAPO-34 surface.

On the addition of 15, 30, 45, and 60 m/uc of chloromethane at room temperature into the IR reactor, the bridged hydroxyl bands at 3625 and 3598 cm^{-1} decrease in intensity at a chloromethane loading of 15 m/uc and disappear completely at higher system loadings of chloromethane. Simultaneously, four new and sharp bands appear at 2960, 2863, 1442, and 1347 cm^{-1}, attributed to the antisymmetric or symmetric stretching and bending vibrations of methyl group of CH_3Cl, respectively, indicating the adsorption of chloromethane molecules on the catalyst. The very broad and intense band that can be decomposed by a Winspec program to two overlapped components centered at 3299 and 3270 cm^{-1} is also observed and can be attributed to the interaction of CH_3Cl with the two bridged hydroxyl groups. (Fig. 4Ac and d show even more clearly the existence of two components). The interaction with CH_3Cl shifts the two hydroxyls at 3625 and 3598 cm^{-1} to lower wavenumbers. This observation suggests the accessibility of both two bridging Si(OH)Al groups to chloromethane molecules. Kazansky et al. [22] performed the adsorption of CH_3I on SAPO-34 and found that the high-frequency (3625 cm^{-1}) and low-frequency (3600 cm^{-1}) bands disappeared after adsorption of CH_3I, giving a very broad band at 3280 cm^{-1}. Kazansky et al.'s observation of only one broad band instead of the two components seen in the present study is very likely due to the different resolution of the IR apparatus used in the two studies. It is well known that the extent of the shift depends on the acidity of the hydroxyl (the more strongly acidic the hydroxyl, the greater the shift), and so the value of the shift has been often used to evaluate the acid strength of a hydroxyl group of solids. The evaluation of the shift value gives quite similar values of about 326 and 328 cm^{-1} for the hydroxyls at 3625 and 3598 cm^{-1}, respectively, signifying that both types of OH groups exhibit similar acidic properties, confirming the prediction made by Kazansky et al. [22] and Angyan et al. [25]. These values are lower than those observed for HZSM-5 (412 cm^{-1}), HBeta (427 cm^{-1}), and HMOR (415 cm^{-1}), but similar to those found for HEMT (322 cm^{-1}) and HY (330 cm^{-1}), indicating that our SAPO-34 has a medium acid strength. The results demonstrate that chloromethane can be used as an efficient probe molecule for the evaluation of acid strength of solids, as described previously [16].

Two kinds of bridged hydroxyls of SAPO-34, with absorption bands at 3625 and 3598 cm^{-1} due to their accessibility to and interaction with CH_3Cl, could be the active sites in the chloromethane conversion. Comparing the spectra of chloromethane adsorption, the spectra given in Fig. 4Ab indicate that a system loading of 15 m/uc cannot consume all of the active sites of the catalyst. With the appearance of four peaks at 2960, 2863, 1442, and 1347 cm^{-1}, representing the absorption bands of methyl group of CH_3Cl, the bridged hydroxyl bands decrease in intensity but can still be readily observed with lowered intensity. Because all of the chloromethane molecules introduced are adsorbed into the SAPO-34 pore system, no free chloromethane can be observed in the gas phase (Fig. 4Bb). On increasing the system loading of chloromethane to ⩾30 m/uc (Fig. 4Ac–Ae), the absorption bands stemming from the bridged hydroxyls disappear, indicating that all of the active sites of the catalyst have been occupied by the chloromethane. The free chloromethane molecules (CH_3– at 2970, 2880, 1456, and 1348 $cm^{-1}$and C–Cl at 745 and 711 cm^{-1}) are simultaneously detected in gas phase of the IR cell (Fig. 4Bc–Be). The wavenumbers of these bands are slightly different than those of the adsorbed phase. With the effect of Fermi resonance, the absorption bands in gas phase spectra appear with split bands. The intensity of these bands increases with increasing system loading of chloromethane.

3.2.2. Effect of reaction temperature on the conversion of chloromethane

Fig. 5A gives the spectra of adsorption and conversion of chloromethane with a system loading of 45 m/uc over SAPO-34 at different temperatures. Reaction performed at 250 and 300 °C for 15 min (Fig. 5Ac and Ad) produces no significant change in the IR spectrum, meaning that no conversion occurs below 300 °C. Some interesting and relevant changes appear starting at 350 °C (Fig. 5Ae), indicating that the conversion may start from this temperature. From 350 to 450 °C, the intensities of the four peaks at 2960, 2863, 1442, and 1347 cm^{-1} due to the methyl group of CH_3Cl decrease, suggesting that the transformation is occurring. At the same time, with the consumption of chloromethane molecules, the bands at 3299 and 3270 cm^{-1}, due to chloromethane interaction with the active sites, also lose intensity. A band at around 1669 cm^{-1} appears at 350 °C and becomes remarkable with increasing temperature. This band

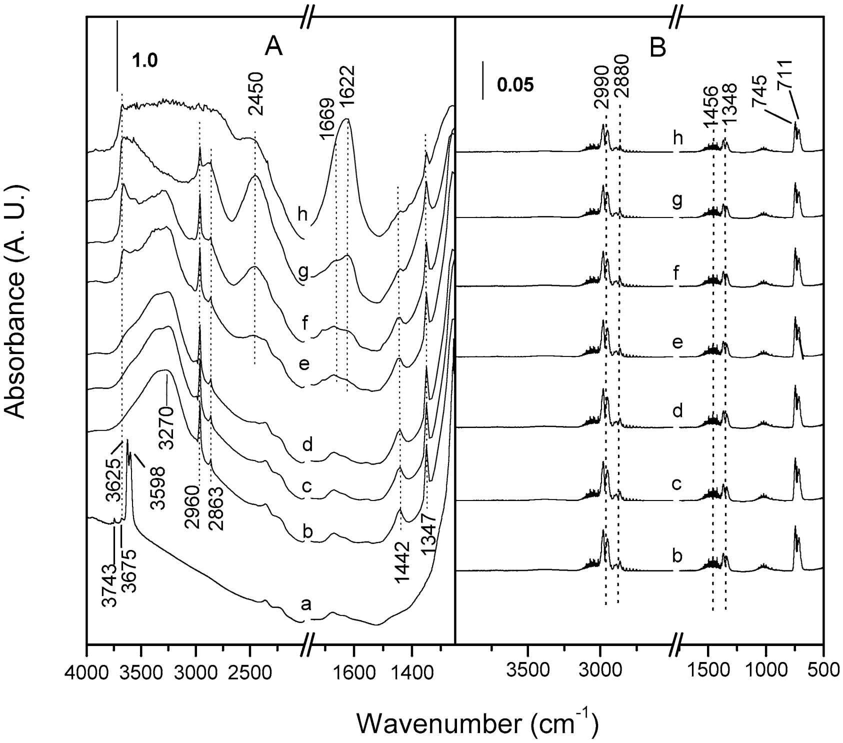

Fig. 5. FTIR spectra of chloromethane adsorption (45 m/uc) and conversion at different temperatures (°C): (A) adsorption phase on SAPO-34, (B) gas phase. (a) Activated SAPO-34 at 450 °C and reaction at (b) RT, (c) 250, (d) 300, (e) 350, (f) 400, (g) 450, (h) 500 °C for 15 min.

Table 1
Wavenumbers and assignments of IR bands of chloromethane conversion over SAPO-34

Wavenumbers (cm^{-1})	Assignments	Wavenumbers (cm^{-1})	Assignments
2960 (2970[a])	υ(C–H)as of $-CH_3$	1602	$\upsilon(C{=}C)_n$ of alkene
2920	υ(C–H)as of $-CH_2-$	1572	υ(C–C) of aromatic and polymer
2878	$\upsilon(OH) \pm \upsilon(OH\cdots Cl)$		
2870	υ(C–H)s of $-CH_3$	1442 (1456[a])	δ(C–H)as of $-CH_3$
2863 (2880[a])	υ(C–CH)s of $-CH_3$	1378	δ(C–H)s of $-CH_3$
2450	$\upsilon(OH) \pm \upsilon(OH\cdots Cl)$	1347 (1348[a])	δ(C–H)s of $-CH_3$
1669	υ(C=C) of alkene	950[a]	γ(C–H) of $-CH_2-$
1622	$\upsilon(OH) \pm \upsilon(OH\cdots Cl)$	747, 711[a]	υ(C–Cl) of $-CH_3$

[a] Absorbance in gas phase.

can be attributed to the stretching vibration of C=C, indicating the generation of alkenes from chloromethane conversion over the surface of the catalyst. Attributions of all of the vibration bands observed for the products of conversion are given in Table 1.

Based on the study of a series of protonic zeolites, negatively charged chlorine atoms of chloromethane can interact with hydrogen atoms of hydroxyls in a hydrogen-bond form, and the positively charged carbon atoms can also interact with the oxygen atoms of zeolite framework to give a surface methoxy species and HCl, as demonstrated by Murray and others [10,14,16].

It is noteworthy that a series of broad bands appear at around 2878, 2450, and 1622 cm^{-1} (with the band at 2878 cm^{-1} overlapping bands at 2960 and 2863 cm^{-1}) and increase in intensity with increasing reaction temperature. These three broad bands may come from the H-bonding complex and be attributed to the perturbed OH vibration, because they are quite similar to the triplet A, B, C bands of the hydroxyl group reported previously [28,29]. Usually, for the H-bonding complex, the A–B–C pattern with broad and intense absorbance at around 2800, 2400, and 1700 cm^{-1} is caused by a Fermi resonance between out-of-plane deformation vibration of bridged OH group and the perturbed hydrogen-bound OH group due to O–H···X–H formation.

The observation of a triplet A–B–C pattern as the conversion occurs signifies that HCl is immediately generated from the dehalogenation of chloromethane with the reaction. The strong H-bond complex (A–B–C pattern at 2878, 2450, and 1622 cm^{-1}) is due to the strong interaction between Si(OH)Al and HCl.

Although a large H-complex family has been studied, the explanation for HCl adsorption on the zeolite surface remains obscure. Ozin [30] studied HX adsorption over NaY and HY and considered the bands of 2800 and 2400 cm^{-1} as being a red-shifted OH group and a blue-shifted HCl group (O–H···X–H). In Kiricsi's [31] work on the adsorption and reaction of methyl chloride on acidic, neutral, and basic zeolites, even though HCl was also considered as one of main products of the reaction, absorbance was not reported in the zone of 2800–1800 cm^{-1}, similar to other work [9,10] carried out on chloromethane transformation by means of FTIR on a series of zeolite catalysts (Beta, Y, MOR, EMT, and ZSM-5).

In the study reported here, besides the generation of H-complex with A–B–C patterns caused by HCl adsorption, another quite interesting and important fact to note is that the intensity of absorption at 3675 cm^{-1} increases significantly with the occurrence of the reaction at 350 °C (Fig. 5Ae). For the activated sample, this peak is assigned to the P–OH of SAPO-34. Its increasing intensity indicates the generation of a large amount of P–OH during chloromethane conversion, possibly from HCl adsorption on the aluminophosphate framework. The dissociative HCl adsorption on the framework may break the Al–O–P bond and produce a new bonding of P–OH and AlCl. Similar dissociative HCl adsorption was previously reported in a study of HCl adsorption on an Al_2O_3 surface [32]. In the earlier study by Lunsford, no new hydroxyl groups were found when Mg, P-modified ZSM-5 was exposed to HCl [11]. When chloromethane transformation was carried out in cationic zeolite, a hydroxyl group appeared after the reaction [10].

The foregoing observations (i.e., A–B–C triplet pattern and increased intensity of P–OH groups) reveal that the elimination of HCl from CH_3Cl is the first step in chloromethane conversion and the precursor of the C–C bond formation. This is in complete agreement with previous reports by different groups [10,14].

On a further temperature increase to 500 °C (Fig. 5Ah), a larger band appears in the hydroxyl absorption zone (3700–3000 cm^{-1}). This can be explained by the interaction of the bridged hydroxyls with different alkenes. The absorbance of hydroxyls becomes very complicated for this reason.

The gas phase in the IR cell at different temperatures were also analyzed (Fig. 5B). With increasing the reaction temperature, the intensity of the bands of C–Cl, appearing as split bands at 745 and 711 cm^{-1}, decreases, indicating that some chloromethane molecules in the gas phase has been consumed during the reaction. No other new species can be found in the gas phase, suggesting that the reaction may occur mainly over the surface of the catalyst, and that the products result from the conversion of adsorbed chloromethane. After conversion, the products (e.g., HCl and alkenes) are still adsorbed over the catalyst surface and can be detected only as the adsorbed species.

3.2.3. *Effect of chloromethane system loading on the conversion of chloromethane studied by FTIR*

A detailed FTIR study was performed to gain a better understanding of the reaction mechanism. Different amounts of chloromethane were introduced into the IR cell containing SAPO-34 wafers. The IR cell temperature was increased to 450 °C and kept there for 5, 15, 30 and 60 min, at which points the spectrum was recorded. The spectra of the adsorbed species on catalyst and the gas phase with system chloromethane loading of 15, 30, 45, and 60 m/uc are depicted in Figs. 6–9.

In the spectra of chloromethane loading of 15 m/uc (Fig. 6), after 5 min of reaction at 450 °C, the bands at 3299 and 3270 cm^{-1} (due to the interaction of two types of Si(OH)Al with CH_3Cl) and the bands at 2960, 2863, 1442, and 1347 cm^{-1} (stemming from CH_3Cl) significantly decrease in intensity, indicating the conversion of chloromethane. The simultaneous appearance of the band at 1378 cm^{-1}, attributed to the

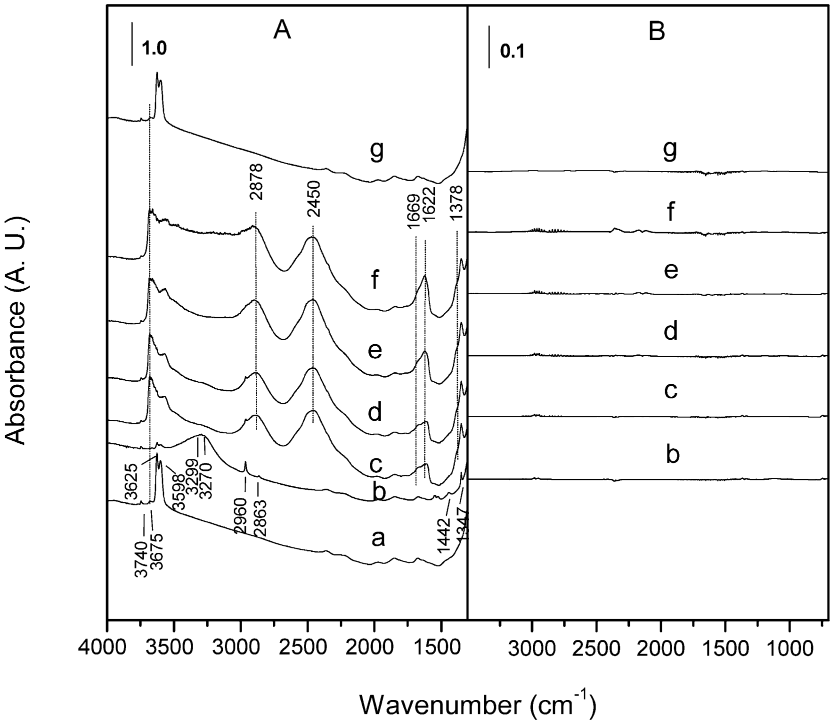

Fig. 6. FTIR spectra of chloromethane adsorption (15 m/uc) and conversion at 450 °C: (A) adsorption phase on SAPO-34, (B) gas phase. (a) Activated SAPO-34, CH_3Cl adsorption at RT (b) and reaction at 450 °C for 5 (c), 10 (d), 15 (e), 60 min (f), and evacuation at 150 °C for 60 min (g).

methoxyl group, and the band at 1669 cm^{-1}, from the adsorbed C=C species, proves that dehalogenation to give HCl and surface methoxy groups and C–C bond formation occur at the beginning of the reaction. The triple bands at 2878, 2450, and 1622 cm^{-1} also appear, suggesting H-bond formation between bridged hydroxyl with HCl as a product of the dehalogenation of chloromethane. The intensity of P–OH (band at 3675 cm^{-1}) increases visibly with conversion and HCl adsorption, as discussed in Section 3.2.2.

With prolonging the reaction time, the bands representing the methoxyl group and C=C slightly increase in intensity, suggesting that more chloromethane molecules are transformed to products. A broad absorbance appears progressively at 3000–3600 cm^{-1}, which may be attributed to the bridged hydroxyls interacting with the formed alkenes. During the reaction period, nothing can be observed in the spectra of the gas phase of the IR cell; all of the reactants and products are adsorbed on the catalyst surface. Desorption at 150 °C for 60 min in vacuum can eliminate all of the species adsorbed on catalyst and completely restore all of the bridged hydroxyls. P–OH also recovers its initial intensity. There is no difference between the spectra in Fig. 6Aa and Ag, indicating good catalyst regeneration and stability. In this quite interesting reversible process, breakage of Al–O–P bonds by adsorption of HCl, a main product of the reaction, gives a large amount of P–OH groups and AlCl, and the regeneration of Al–O–P bonds occurs after removal of HCl.

Product generation is similar at chloromethane loadings of 15 and 30 m/uc (Fig. 7). It is easily seen a broad absorbance at 2878 cm^{-1} overlaps with peaks at 2960, 2920, and 2870 cm^{-1}. These three peaks may be attributed to the ethoxyl species (2960 and 2870 cm^{-1} from CH_3– and 2920 cm^{-1} from –CH_2–), and ethylene probably will be liberated from this species. These bands are also observed when HZSM-5 was used as the catalyst for chloromethane transformation [33]. These bands provide direct proof of the formation of alkoxyl surface species as proposed earlier [10,14,15]. The high intensity of absorption at 1669 cm^{-1} indicates the generation of more alkenes at a reaction time of 60 min. With a reaction time of 5 min, a new band at 1572 cm^{-1} appears and could be attributed to the vibration of the aromatic or polymerized $(C{=}C)_n$, showing the possible occurrence of alkene polymerization or coke formation when the conversion is carried out at relatively high chloromethane system loading. From the gas-phase spectra in Fig. 7B, chloromethane in gas phase can be detected at a loading of 30 m/uc. The absorbances at 2970, 2880, 1456, and 1348 cm^{-1} appear as split bands. The bands at 745 and 711 cm^{-1} decrease in intensity with increasing reaction time but remain observable even after prolonged reaction times. No vibration bands of HCl or alkenes are detected in the gas phase. Not all of the framework hydroxyls can be regenerated by desorption at 150 °C for 60 min in vacuum, indicating that some adsorbed species remain on the catalyst surface.

Increasing the chloromethane system loading to 45 m/uc, the spectra in Fig. 8 are similar to those obtained with the loading of 30 m/uc, whereas the conversion is enhanced compared with at lower chloromethane loadings. Reaction at 450 °C brings about intensified bands of Si(OH)Al perturbed with adsorbed HCl; the broad band at 3000–3500 cm^{-1}, caused by the adsorption of alkenes on hydroxyl groups, also shows high intensity, indicating generation of large amounts of alkenes. The vibration bands of C=C (1669 cm^{-1}) and $(C{=}C)_n$ (1572 cm^{-1}) appear, and the latter becomes more and more remarkable. Still

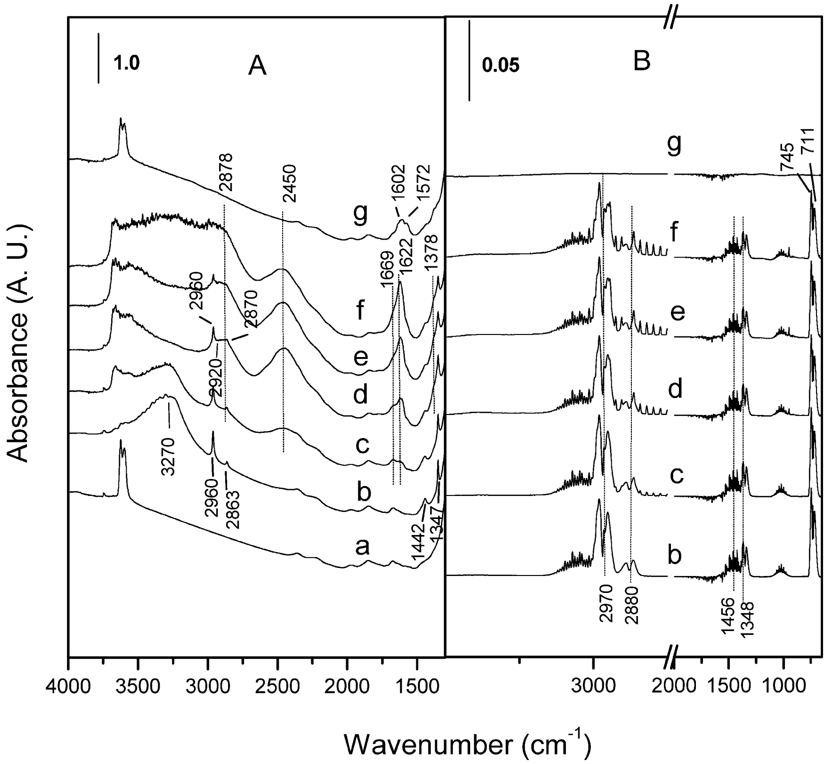

Fig. 7. FTIR spectra of chloromethane adsorption (30 m/uc) and conversion at 450 °C: (A) adsorption phase on SAPO-34, (B) gas phase. (a) Activated SAPO-34, Reaction at RT (b) and at 450 °C for 5 (c), 10 (d), 15 (e) and 60 min (f) and evacuation at 150 °C for 60 min (g).

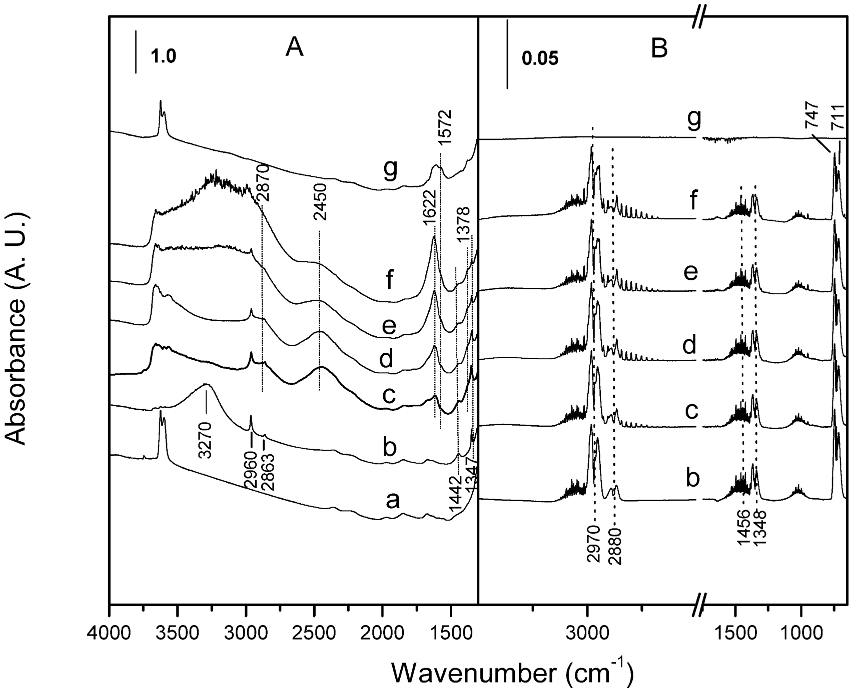

Fig. 8. FTIR spectra of chloromethane adsorption (45 m/uc) and conversion at 450 °C: (A) adsorption phase on SAPO-34, (B) Gas phase. (a) Activated SAPO-34, CH_3Cl adsorption at RT (b) and reaction at 450 °C for 5 (c), 10 (d), 15 (e) and 60 min (f), and evacuation at 150 °C for 60 min (g).

no vibration bands of the products can be detected from the gas-phase spectra of the IR cell.

On a further increase in system chloromethane loading to 60 m/uc (Fig. 9), the reaction results in a higher conversion rate. The band at 1342 cm^{-1}, the vibration of the other hydrocarbon band of CH_3Cl, rapidly decreases in intensity, and the band of the methoxy group at 1378 cm^{-1} sharply increases in height. This finding suggests an accelerated chloromethane conversion compared with that at lower chloromethane loadings. The absorption at 1572 cm^{-1} becomes more prominent,

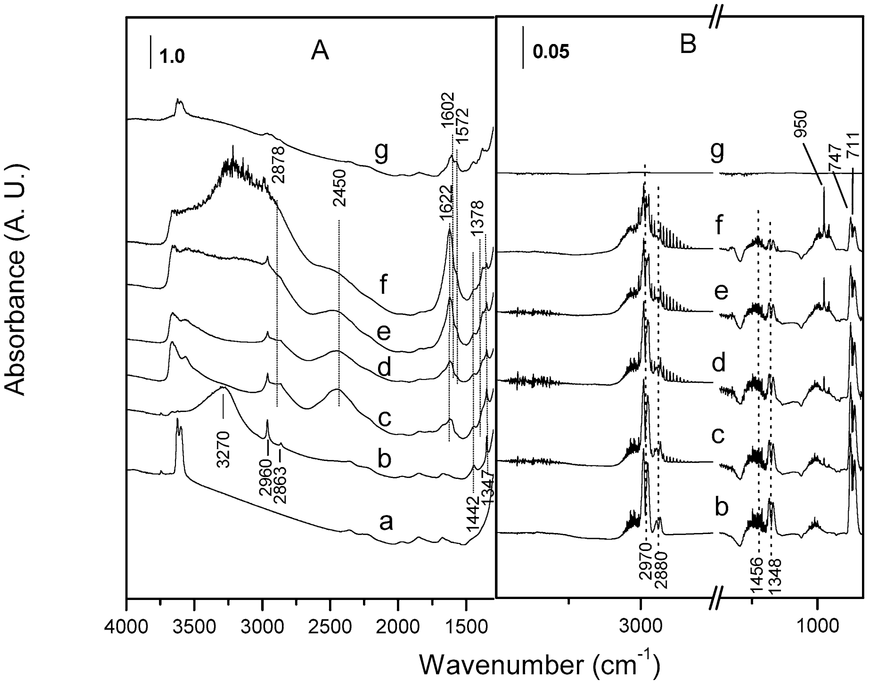

Fig. 9. FTIR spectra of chloromethane adsorption (60 m/uc) and conversion at 450 °C: (A) adsorption phase on SAPO-34, (B) gas phase. (a) Activated SAPO-34, CH_3Cl adsorption at RT (b) and reaction at 450 °C for 5 (c), 10 (d), 15 (e) and 60 min (f), and evacuation 150 °C for 60 min (g).

meaning greatly enhanced polymerization. High pressure in the gas phase may thus favor chloromethane conversion to HCl and alkenes as well as further reactions, such as oligomerization, polymerization, and alkylation. From the gas-phase spectra of the IR cell, the vibration bands of C–H at 2970 and 2880 cm^{-1} and of C–Cl at 745 and 711 cm^{-1} sharply decrease in intensity with increasing reaction time, signifying the consumption of chloromethane molecules in the gas phase on reaction. This finding is consistent with the change of the band at 1347 cm^{-1} in Fig. 9A. It is notable that a new band at 950 cm^{-1} appears in the gas-phase spectra at a reaction time of 5 min, and that its intensity increases with time. This band may come from the –CH_2– group of CH_3CH_2Cl, which results from the further reaction between the products of ethylene and HCl or an intermediate, such as carbene, with CH_3Cl, as proposed previously [10]. The intensity of hydroxyls is quite low after desorption (Fig. 9Ag) compared with that before the reaction (Fig. 9Aa), and some adsorbed species remain on the catalyst surface, inhibiting the complete regeneration of hydroxyl groups.

The spectra depicted in Figs. 6–9 show that the conversion of chloromethane is dependent on the amount of system chloromethane loading. The vibration at 747 cm^{-1} in the gas-phase spectra due to the vibration of C–Cl of CH_3Cl has been tested, and its intensity is used to follow the consumption of chloromethane over time at different chloromethane loadings. Fig. 10 shows the variation in intensity of this band at different loadings.

For a 15 m/uc chloromethane loading, no chloromethane in the gas phase is observed as a function of reaction time. Comparing the intensity changes at system loadings of 15, 30, 45, and 60 m/uc reveals that the decreased intensity of the band at 747 cm^{-1} is more prominent in conversions with higher system chloromethane loadings. This may suggest that at relatively high chloromethane loadings, the reactant in the gas phase can react with the adsorbed species, so the reactant in the gas phase is consumed with the conversion. For conversion at low chloromethane loadings, the reaction may occur only between the adsorbed species on the catalyst surface, even though some chloromethane molecules can be present in the gas phase of the IR reactor.

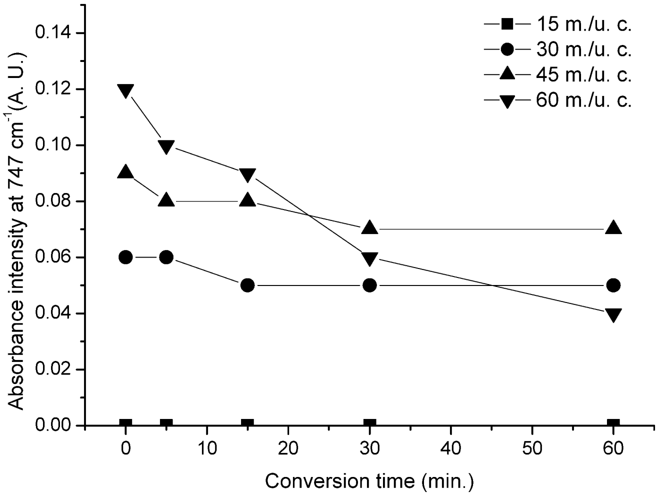

Fig. 10. The intensity change of the band at 747 cm^{-1} in gas-phase spectra after the reaction at 450 °C.

It is also interesting to note that despite the large amount of P–OH groups formed, these groups remain unchanged without interaction with CH_3Cl or products issued from the reaction. This is likely due to their very weak acidity or their inaccessibility.

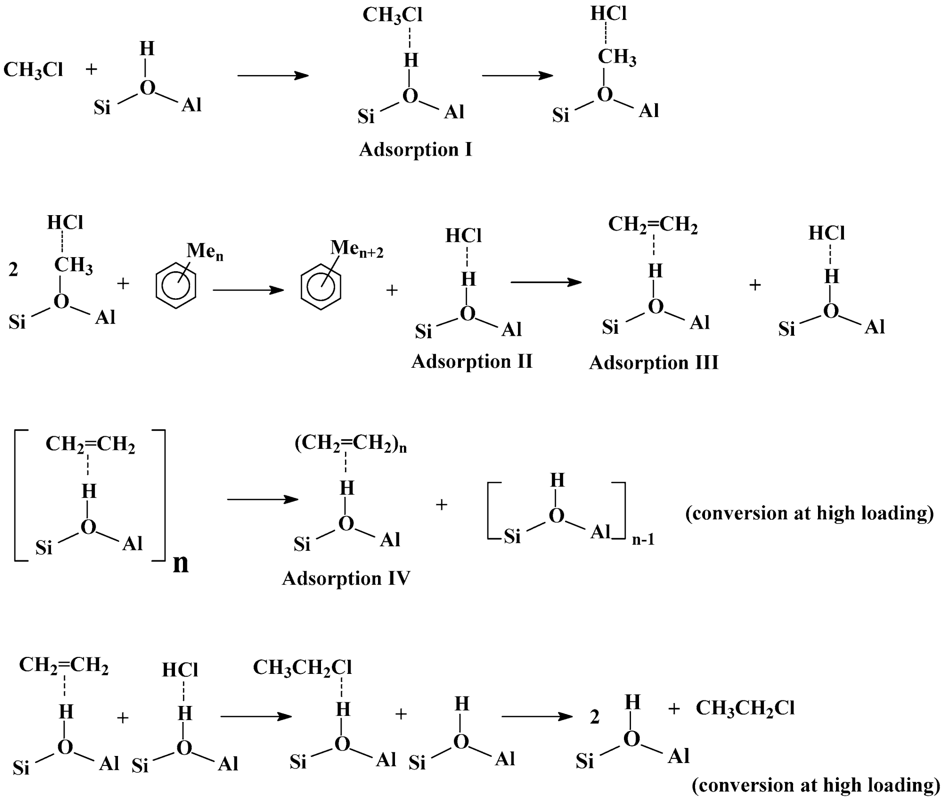

Scheme 1. Adsorption and conversion of chloromethane over SAPO-34.

4. Reaction mechanism

The formation of the triplet A–B–C pattern, the generation of P–OH groups (described in Section 3.2.2 and further confirmed by the results of Section 3.2.3), and the detection of surface alkoxy groups (Section 3.2.3) are the essential findings and clearly demonstrate that the dehalogenation to split HCl and methyl giving surface methoxy groups from CH_3Cl is the first step in chloromethane conversion. This is quite useful for drawing a clear reaction mechanism. In this section we propose a realistic reaction mechanism in a step by step fashion to correlate with all of the observations.

Our FTIR and catalytic testing work using SAPO-34 in chloromethane transformation found alkenes and HCl as the main products. This is quite different from the products given with protonic and cationic zeolites used as catalysts [9,10]. The FTIR results show some special adsorbed species, providing useful information for elucidating the interaction between the active sites with reactant and products. Three shifts of Si(OH)Al caused by three adsorption species can be seen during the adsorption and conversion of chloromethane (see Scheme 1). The interaction between chloromethane and Si(OH)Al induces the shift of hydroxyl bands at 3625 and 3598 cm^{-1} to 3299 and 3270 cm^{-1}, respectively (adsorption I). With chloromethane consumption, H-bond species give the typical A–B–C pattern (2878, 2450, and 1622 cm^{-1}), resulting from the adsorption of HCl (adsorption II). The Si(OH)Al shifts to a broader range of 3000–3500 cm^{-1}, possibly due to the adsorption of alkenes (adsorption III). From these species, we would expect subsequent C–C formation during the process of conversion.

During conversion, most products remain on the surface of SAPO-34 as adsorbed species. It is rather difficult to find products eliminated from the surface and present in the gas phase of the IR cell. After conversion, evacuation was done at 150 °C for 60 min to remove the adsorption species. For all of the spectra, the bands of the H-bond species, O–H$\cdots$X–H, could be removed completely. A new phenomenon was revealed, that the adsorption of HCl on the framework can induce breakage of Al–O–P bonds to generate a large amount of P–OH groups at 3675 cm^{-1} (Figs. 6–9), and that the Al–O–P bonds can be restored by removing the HCl by vacuum. This reversible process was reported previously with the adsorption of NH_3 on SAPO-34 [34], but this paper is the first report of the process during chloromethane conversion. The removal of alkene species over the surface depends on the system chloromethane loading. For a 15 m/uc chloromethane loading, alkenes generated with bands at 1669 cm^{-1} can be removed completely, and the Si(OH)Al bands can regain their initial intensity (Fig. 6Ag). But for system chloromethane loadings of 30, 45, and 60 m/uc, even after evacuation at 150 °C, some adsorbed species can still be seen on the catalyst surface (bands at 1602 and 1572 cm^{-1} in Figs. 7Ag, 8Ag, and 9Ag). These species are expected to be the high-polymerized alkenes, $(C{=}C)_n$ or coke species (adsorption IV). Therefore, the bridged hydroxyls cannot be completely regenerated at 150 °C.

Two mechanisms have been proposed for the transformation of chloromethane to higher hydrocarbons with zeolite as the catalyst; both of these mechanisms consider methoxy the first intermediate and ethoxyl species the second intermediate, with ethylene generated from the ethoxy group [9,10,14,15]. In our study, the FTIR spectra demonstrate the possible existence of these two adsorbed species during the reaction, with the appearance of bands at 1378 and 1669 cm^{-1}, from methoxy and C=C, respectively, proving that for chloromethane transformation over acid catalyst SAPO-34, dehalogenation and subsequent C–C band formation occur as in zeolite catalysts.

The explanations for C–C band formation are quite diverse. In Murray's work, formation of the C–C bond resulted from the methylation of framework-bound CH_2 species with a methyl group from dehalogenated CH_3X [14]. In another mechanism, CH_2 species were more free and could transfer from one framework site to the neighboring methoxy group, and the C–C bond formed from carbene insertion into the C–H bond of this neighboring methoxy group [9,10]. These two mechanisms were considered direct routes for C–C bond formation, whereas the study of Haw and Kolboe proved that the first C–C bond in an MTO reaction may occur in an indirect way, to avoid the high-energy intermediate required in all direct mechanisms [35–37]. A reaction center called the hydrocarbon pool, typically composed of cyclo-organic species, acts as a scaffold for an assembly of light olefins. For chloromethane transformation, even the detection of initial hydrocarbon buildup is difficult, theoretical analysis strongly favors the associative mechanism, with the first C–C bond formation occurring after a methylation step [38]. In our present study of chloromethane transformation over SAPO-34, in catalytic testing, the narrow SAPO-34 window obscures the cyclo-organic products, such as benzene and substituted benzene, in the gas chromatograph. The FTIR study reveals absorbance at 1572 cm^{-1}, which can be attributed to $\upsilon(C–C)_n$ of aromatic species. This band is very obvious for the transformation with high system chloromethane loadings, indicating that the cyclonic reaction center, which has been found by NMR and MASS in the MTO reaction [35–37], may also form in the cage of SAPO-34 and cannot escape from the window of the pores. A possible pathway of first C–C bond formation is given in Scheme 1. The first reaction center, such as methylbenzene, is assumed to be present in the cage of SAPO-34, possibly from the initial buildup with methoxy species or trace coke deposition from incomplete calcination. Subsequent methylation from adsorbed chloromethane leads to the formation of multimethylbenzene and HCl; then the multibenzene eliminates an ethylene. Once ethylene is synthesized, additional methylbenzene formation will continue through oligomerization and cyclization of olefins followed by hydrogen transfer.

The present study shows a very interesting trend from varying the system chloromethane loadings. A high chloromethane loading (meaning a relatively high reactant pressure in the reaction cell) favors chloromethane conversion and product generation. Usually the conversion is associated with the catalyst active sites. For the SAPO-34 catalyst studied here, the bridged hydroxyl Si(OH)Al is considered as an active site. Fig. 4 shows that a chloromethane loading of 15 m/uc is insufficient to occupy all of the active catalyst sites, and the bands of Si(OH)Al at 3625 and 3598 cm^{-1} can still be observed. With loadings $\geqslant 30$ m/uc, the bands of Si(OH)Al disappear, and the bands of gaseous chloromethane appear in the gas-phase spectra (CH_3– of CH_3Cl at 2970, 2880, 1456, and 1348 $cm^{-1}$and C–Cl at 745 and 711 cm^{-1}). During the process of chloromethane transformation, the intermediate of alkoxy groups and products of alkenes and HCl occupy the active sites and may delay the continued conversion. Interestingly, however, high conversion rates occur at higher loadings. It is supposed that most of the reaction center methylbenzenes result from secondary reaction of ethylene, as discussed earlier; that high system chloromethane loadings may favor the generation of large amounts of ethylene in the next step; and that more methylbenzene can be synthesized at the reaction center. The presence of dense hydrocarbon pools in the cage will speed up the conversion of chloromethane, so the sharp consumption of gas-phase chloromethane can be observed.

Comparing the spectra of chloromethane at loadings of 15, 30, 45, and 60 m/uc reveals differences in C=C and $(C=C)_n$ formation. At low chloromethane loading, C=C with a band at 1669 cm^{-1} appears as the main absorbance; at higher system loadings, the band at 1572 cm^{-1} due to aromatic or polymerized $(C=C)_n$ increases in intensity and becomes more prominent. After the polymerization of alkenes (i.e., consumption of adsorbed alkenes), some Si(OH)Al sites are no longer occupied and once again are available for the reactant in the gas phase. At a system loading of 60 m/uc, the band of CH_3CH_2Cl clearly appears in the gas-phase spectra, indicating that high loading also improves the further reaction of $CH_2=CH_2$ and HCl or of CH_2 with CH_3Cl. The giving off of CH_3CH_2Cl from the catalyst surface may be another possible route of adsorption and conversion of chloromethane on active sites.

5. Conclusion

SAPO-34 is a very active, selective, and promising catalyst for the production of light alkenes from chloromethane transformation. In the temperature range of 350–500 °C, 70–80% selectivity of light alkenes can be obtained. Adsorption and dehalogenation of CH_3Cl and formation of C–C subsequently occur. Alkenes and HCl appear as the main products, which remain on the catalyst surface as adsorbed species. The dissociative adsorption of HCl on Al–O–P generates new P–OH, whereas the removal of HCl can restore the Al–O–P bonds. This reversible process is reported here for the first time with SAPO-34 under a reaction process. Chloromethane conversion is related to system chloromethane loading, with higher loadings inducing higher conversion rates. More hydrocarbon pool formation and a further reaction of alkenes, such as alkene polymerization and CH_3CH_2Cl formation, are the reason for the rapid conversion.

Acknowledgments

This work was realized in the framework of a European Inter Reg III program (France–Wallonie–Flandre, FW-2.1.5). Y.W. thanks the University of Namur for a postdoctoral scholarship.

References

[1] C.D. Chang, A.J. Silvestri, J. Catal. 47 (1977) 249.
[2] C.D. Chang, W.H. Lang, A.J. Silvestri, US Patent 3,998,898 (1976).
[3] C.D. Chang, W.H. Lang, US Patent 3,899,544 (1975).
[4] C.D. Chang, Catal. Rev. Sci. Eng. 25 (1983) 1.
[5] G.A. Olah, B. Gupta, M. Farina, J.D. Felberg, W.M. Ip, A. Husain, R. Karpeles, K. Lammertsma, A.K. Melhotra, N.J. Trivedi, J. Am. Chem. Soc. 107 (1985) 7097.
[6] C.E. Taylor, R.P. Noceti, Stud. Surf. Sci. Catal. 36 (1988) 483.
[7] C.E. Taylor, R.R. Anderson, J.R. D'Este, R.P. Noceti, Stud. Surf. Sci. Catal. 130 (2000) 3633.
[8] P. Lersch, F. Bandermann, Appl. Catal. 75 (1991) 133.
[9] D. Jaumain, B.L. Su, Stud. Surf. Sci. Catal. 130 (2000) 1607.
[10] D. Jaumain, B.L. Su, J. Mol. Catal. A: Chem. 197 (2003) 263.
[11] Y. Sun, S.M. Campbell, J.H. Lunsford, G.E. Lewis, D. Palke, L.-M. Tau, J. Catal. 143 (1993) 32.
[12] J.B. Nicholas, J.F. Haw, J. Am. Chem. Soc. 120 (1998) 11804.
[13] G.H. Hutchings, R. Hunter, Catal. Today 6 (1990) 279.
[14] D.K. Murray, J.-W. Chang, J.F. Haw, J. Am. Chem. Soc. 115 (1993) 4732.
[15] D.K. Murray, T. Howard, P.W. Goguen, T.R. Krawietz, J.F. Haw, J. Am. Chem. Soc. 116 (1994) 6354.
[16] D. Jaumain, B.L. Su, Catal. Today 73 (2002) 187.
[17] J. Liang, H.Y. Li, S.Q. Zhao, W.G. Guo, R.H. Wang, M.L. Ying, Appl. Catal. 64 (1990) 31.
[18] Y. Xu, C.P. Grey, J.M. Thomas, A.K. Cheetham, Catal. Lett. 4 (1990) 251.
[19] T. Inui, Stud. Surf. Sci. Catal. 105 (1997) 1441.
[20] B.M. Lok, C.A. Messina, R.L. Patton, R.T. Gajek, T.R. Cannan, E.M. Flanigen, US Patent 4,440,871 (1984).
[21] J. Tan, Z. Liu, X. Bao, X. Liu, X. Han, C. He, R. Zhai, Microporous Mesoporous Mater. 53 (2002) 97.
[22] S.A. Zubkov, L.M. Kustov, V.B. Kazansky, I. Girnus, R. Fricke, J. Chem. Soc. Faraday Trans. 87 (1991) 897.
[23] R. Vomscheid, M. Briend, M.J. Peltre, D. Barthomeuf, P.P. Man, J. Chem. Soc. Faraday Trans. 91 (1995) 3281.
[24] M. Briend, R. Vomscheid, M.J. Peltre, P.P. Man, D. Barthomeuf, J. Phys. Chem. 99 (1995) 8270.
[25] Y. Jeanvoine, J.G. Angyan, G. Kresse, J. Hafner, J. Phys. Chem. B 102 (1998) 5573.
[26] L. Smith, A.K. Cheetham, R.E. Morris, L. Marchese, J.M. Thomas, P.A. Wright, J. Chen, Science 271 (1996) 799.
[27] L. Smith, A.K. Cheetham, L. Marchese, J.M. Thomas, P.A. Wright, J. Chen, E. Gianotti, Catal. Lett. 41 (1996) 13.
[28] A.G. Pelmenschikov, R.A. van Santen, J. Phys. Chem. 97 (1993) 10678.
[29] A.G. Pelmenschikov, J.H.M.C. van Wolput, J. Janchen, R.A. van Santen, J. Phys. Chem. 99 (1995) 3612.
[30] G.A. Ozin, S. Ozkar, G.D. Stucky, J. Phys. Chem. 94 (1990) 7562.
[31] Z. Konya, I. Hannus, I. Kiricsi, Appl. Catal. B 8 (1996) 391.
[32] J.W. Elam, C.E. Nelson, M.A. Tolbert, S.M. George, Surf. Sci. 450 (2000) 64.
[33] X.R. Xia, Y.L. Bi, T.H. Wu, K.J. Zhen, Catal. Lett. 33 (1995) 75.
[34] R. Vomscheid, M. Briend, M.J. Peltre, D. Barthomeuf, P.P. Man, J. Chem. Soc. Faraday Trans. 91 (1995) 3281.
[35] H. Fu, W. Song, J.F. Haw, Catal. Lett. 76 (2001) 89.
[36] B. Arstad, S. Kolboe, Catal. Lett. 71 (2001) 209.
[37] B. Arstad, S. Kolboe, J. Am. Chem. Soc. 123 (2001) 8137.
[38] S. Swelle, S. Kolboe, U. Olsbye, O. Swang, J. Phys. Chem. B 107 (2003) 5251.